Proceedings of the 17th World Congress
The International Federation of Automatic Control
Seoul, Korea, July 6-11, 2008

Two-input Two-output Laboratory-scale Temperature System Based on Peltier Modules ⋆

Péricles R. Barros * **George Acioli Júnior** *
João B. M. dos Santos *

* *Departamento de Engenharia Elétrica, Universidade Federal de Campina Grande, Cx.P. 10105, Campina Grande, PB - BRAZIL.*
e-mail:
prbarros@dee.ufcg.edu.br,[georgeacioli,joaobatista]@ee.ufcg.edu.br

Abstract: A laboratory-scale temperature system for Control and Automation courses is presented. The system is a coupled two-input two-output process which use peltier modules for temperature control. This paper describes the laboratory-scale system in details. A linear dynamic model of the thermoelectric cooler including the heat sink and the cooling-load heat exchanger is developed and experiments are shown which illustrate the use of the system.

Keywords: TITO system; Temperature Control; Laboratory education; PID control; System Identification; Thermoelectric systems.

1. INTRODUCTION

A Peltier module is composed of thermoelectric couples, connected electrically in series and thermally in parallel, and integrated between two ceramic plates. These plates form the cold and hot surfaces and provide mechanical integrity and high electrical insulation from the heat sink and body to be cooled (ichi Uemura [1995]). This module has two terminals to which electrical current is enforced with the purpose of converting electrical energy into a temperature gradient - this thermoelectric phenomena was discovered by Peltier in 1834 and is called Peltier effect.

A thermoelectric couple consists of n- and p-type semiconductor material. Thermoelectric refrigeration is achieved when a direct current is passed through one or more pairs of n- and p-type semiconductor materials. This can occurs in cooling or heating mode. In the cooling mode, direct current passes from the n- to p-type semiconductor material and in heating mode the direction of the current is inverted (Riffat and Ma [2003]).

Another thermoelectric phenomena is called Seebeck effect and it is the inverse of the Peltier effect. A temperature differential between the surfaces of the module generates the Seebeck voltage. The constant that relates this voltage and the temperature differential is called Seebeck coefficient. The product of the Seebeck coefficient and the absolute temperature of the semiconductor material define the Peltier coefficient which controls the peltier effect.

The advent of semiconductor materials enable to use the Peltier effect for a wide variety of thermoelectric refrigeration applications. Peltier modules should be connected with heat exchangers to dissipate heat, which consist of thermoelectric systems. These has been frequently used for the cooling of electronic devices such as CPU, infrared sensors and refrigerators (Goldsmid [1986]). Usually, the temperature at the cold side of the peltier module needs to be maintained at a stable value under variable hot-side and environment temperatures. This relies on a good temperature control technique.

The dynamic behavior of a thermoelectric system results in a complex model that is highly nonlinear. It occurs due to the temperature dependence of physical properties, the resistive heat, and the Peltier effect as can be seen in (Huang and Duang [2000]). Linearization and model reduction usually results in a second order model (without including the actuator and sensor dynamics).

In this paper, a laboratory-scale system using peltier modules for experimental temperature control is described. The laboratory-scale system presented here is a coupled two-input two-output (TITO) process. This system is used in Control and Automation courses at the DEE/UFCG (Departamento de Engenharia Elétrica/Universidade Federal de Campina Grande). The laboratory gives students the opportunity to solve control problems and integrate theoretical knowledge obtained at lectures with practical experience, where the role and relevance of each concept becomes evident. Experiments performed in the laboratory system for teaching students in modeling, continuous-time identification and PI/PID controller design are presented here.

This paper is organized as follows. In section 2, the laboratory-scale temperature system is described. In section 3, a linear dynamic model of the thermoelectric cooler presented in literature is reviewed. In section 4, the experiments performed in the laboratory system are described. In section 5, the experiments results are presented and, finally, conclusions are presented in Section 6.

⋆ This work was supported in part by the CAPES (Coordenação de Aperfeiçoamento de Pessoal de Nível Superior) and CNPq (Conselho Nacional de Desenvolvimento Científico e Tecnológico).

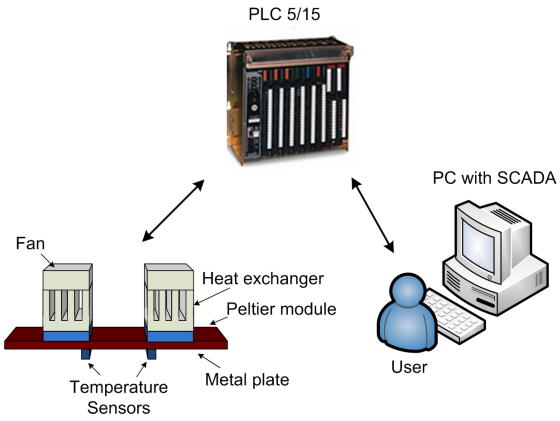

Fig. 1. Laboratory-scale System Overview

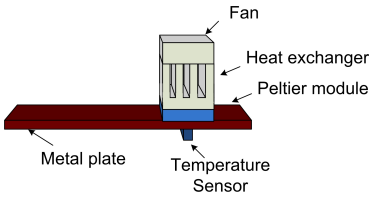

Fig. 2. SISO configuration with smaller delay

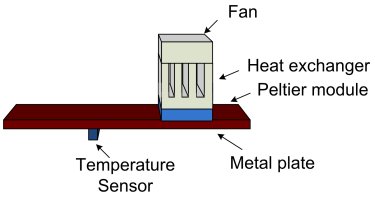

Fig. 3. SISO configuration with larger delay

2. LABORATORY-SCALE SYSTEM DESCRIPTION

The laboratory-scale system (shown in Figure 1) consists of two peltier modules, two LM35 temperature sensors, a metal plate, two heat exchangers, two fans, a PLC (Programmable Logic Controller) and a PC with SCADA (Supervisory Control And Data Acquisition). The peltier modules act as heat pumpers on two sections of a flat metal plate heat load. The heat exchangers and fans are used to transfer heat from the opposite faces of each peltier module. The process works as a coupled TITO system with temperature varying between 10^oC and 70^oC when operating at a room temperature of around 24^oC. Power is applied using PWM actuators while the temperatures are measured using LM35 sensors.

The system allows the use of single-input single-output (SISO) process with smaller and larger delays, depending on the place the temperature is measured (Figures 2 and 3 respectively). In this system the unused peltier module can be used as a perturbation source. The choice of using two modules and two different measurement points yields in a TITO process (Figure 4). TITO process is the most basic and well-known form of multivariable process. Generally, most industrial processes are multivariable.

The control is implemented in a PLC (Allen-Bradley family 5, series 15) or using Matlab with its OPC (OLE for Process Control) toolbox. To improve the interface

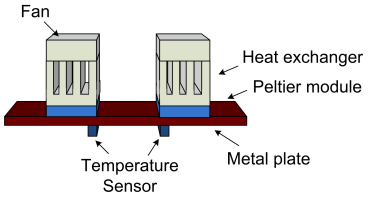

Fig. 4. TITO configuration

between the user and the platform for the PLC , a supervisory window is design using Wonderware's InTouch SCADA software. The entire configuration parameters, monitoring and any change in the process control is done using the supervisory.

The laboratory-scale system is multidisciplinary: it is used in teaching several disciplines during the electrical engineer undergraduate course at UFCG. The undergraduate students have the opportunity to study modeling and simulation techniques, linear control systems design, PLC programming, supervisory design and basic electronics. It is also used in the graduate course, for experimental design and validation of SISO and TITO control techniques, system identification and linear modeling of non-linear process.

This system allows to use the peltier modules for heating or cooling. That is possible because of the use of two bidirectional PWM actuators which supply peltier modules with electrical current in both directions (from the n- to p-type and from the p- to n-type semiconductor material).

In this paper, three experiments results are presented (Figures 2, 3 and 4): two SISO (identification and control for the two configurations) and one TITO (identification by a sequentially step tests).

3. THE DYNAMIC MODEL

In this section, the dynamic model for a thermoelectric system and the heating dynamic coupling is presented. The structure of the dynamic model is determined from a theoretical derivation using the method of small-signal linearization.

3.1 Governing equations

The heat Q_L is absorbed at the metal plate, conducted to the hot-end plate, and then pumped to the hot side of the peltier module (see Figure 5). Energy balance applied to the cold-end plate and the metal as a whole leads to

$$(M_L C_L + M_C C_C)\frac{dT_L}{dt} = Q_L - Q_k - I\alpha_{pn}T_L \qquad (1)$$

where M_L and C_L is the mass and heat capacity of the metal; M_C and C_C is the mass and heat capacity of the cold-end plate; T_L is the temperature of the cold-end plate; Q_k is the heat conduction at the cold-end boundary of the peltier; I is the applied current to the peltier; α_{pn} is the Seebeck coefficient of thermoelectric material.

Energy balance applied to the thermoelectric material will lead to the relation

$$C\gamma\frac{\partial T(x,t)}{\partial t} = k\frac{\partial^2 T(x,t)}{\partial x^2} - \frac{\tau}{A}I\frac{\partial T(x,t)}{\partial x} + \frac{\rho}{A^2}I^2 \qquad (2)$$

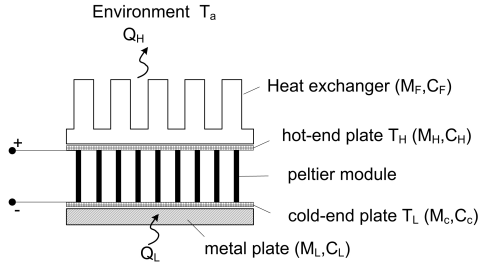

Fig. 5. Schematic Diagram of Thermoelectric System

where C and γ is the mean heat capacity and mean density of the thermoelectric material; $T(x,t)$ is the temperature distribution of the peltier; k is the mean thermal conductivity of the $p-n$ material; τ is the Thomson coefficient defined as $Td\alpha_{pn}/dT$; A is the total cross-sectional area of the thermoelectric material; ρ is the mean electrical resistance of the thermoelectric material.

Similarly, energy balance applied to the heat exchanger and the hot-side plate leads to

$$(M_F C_F + M_H C_H)\frac{dT_H}{dt} = I\alpha_{pn}T_H + Q_o - hA_F(T_H - T_a) \quad (3)$$

where M_F and C_F is the mass and heat capacity of the heat exchanger; M_H and C_H is the mass and heat capacity of the hot-end plate; T_H is the temperature of the hot-end plate; Q_o is the heat conduction at the hot-end boundary of the peltier; h and A_F is the convective heat transfer coefficient and the total heat transfer surface area of the heat exchanger; T_a is the environment temperature.

Eqs. (1), (2) and (3) are the governing equations for the dynamic behavior of a thermoelectric system.

3.2 System dynamic model of the thermoelectric system

A linearization for the governing equations using small-signal analysis is presented in (Huang and Duang [2000]). Applying Laplace transform to linearized version of Eqs. (1)-(3) yields in the transfer function of the perturbed cold-end temperature:

$$\tilde{T}_L(s) = G_I(s)\tilde{I}(s) + G_Q(s)\tilde{Q}_L(s) + G_a\tilde{T}_a(s) \quad (4)$$

where

$$G_I(s) = \frac{N(s)}{sD(s)} \quad (5)$$

$$G_Q(s) = \frac{E_H\sinh(qL) + Akq\cosh(qL)}{D(s)} \quad (6)$$

$$G_a(s) = \frac{AA_F hkq}{D(s)} \quad (7)$$

where

$$N(s) = Akq[\alpha_L\bar{T}_L\cosh(qL) - \alpha_H\bar{T}_H] + \alpha_L\bar{T}_L E_H\sinh(qL)s + \frac{Akq\beta}{C\gamma}[E_H(1-\cosh(pL)) - Akp\sinh(pL)] \quad (8)$$

$$D(s) = AkqE_L\cosh(qL) + E_H E_L\sinh(qL) + AkqE_H\cosh(pL) + A^2k^2pq\sinh(pL) \quad (9)$$

$$p(s) = \frac{\frac{\tau\bar{I}}{A} + \sqrt{\frac{\tau^2\bar{I}^2}{A^2} + 4kC\gamma s}}{2k}$$

$$q(s) = \frac{\frac{\tau\bar{I}}{A} - \sqrt{\frac{\tau^2\bar{I}^2}{A^2} + 4kC\gamma s}}{2k} \quad (10)$$

$$E_L(s) = (M_L C_L + M_c C_c)s + (\tau + \alpha_L)\bar{I} \quad (11)$$

$$E_H(s) = (M_F C_F + M_H C_H)s + hA_F - (\tau + \alpha_H)\bar{I} \quad (12)$$

$$\beta = \frac{2\rho\bar{I}}{A^2} - \frac{\tau(\bar{T}_H - \bar{T}_L)}{AL} \quad (13)$$

Eq. (4) indicates that the cold-end temperature of the thermoelectric cooler T_L is affected by the variations in I, Q_L and T_a. $G_I(s)$, $G_Q(s)$ and $G_a(s)$ are the transfer functions accounting for the system dynamic behavior caused by current, cooling load and ambient temperature variations, respectively.

For a thermoelectric system performed at a constant Q_L and a fixed environment condition, results in system dynamic model for the current input:

$$G_I(s) = \frac{\tilde{T}_L(s)}{\tilde{I}(s)} = \frac{N(s)}{sD(s)} \quad (14)$$

3.3 Plate Temperature Model

Under ideal conditions, the coupling existing between the two thermoelectric modules is described by the heat-diffusion equation. A complete discussion for heating dynamics is presented in (Ljung [1999]).

The heating or cooling power is represented by the input $u(t)$, and the output is represented by $y(t)$ that is the sensor measurement. If $x(t,\xi)$ denotes the temperature at time t, ξ length units from one end of the plate, then

$$\frac{\partial x(t,\xi)}{\partial t} = \kappa\frac{\partial^2 x(t,\xi)}{\partial\xi^2} \quad (15)$$

where κ is the coefficient of thermal conductivity. The heating at the far end means that

$$\frac{\partial x(t,\xi)}{\partial\xi}|_{\xi=L_p} = Ku(t) \quad (16)$$

where K is the hear transfer coefficient and L_p is the plate length. The near end is insulated so that

$$\frac{\partial x(t,\xi)}{\partial\xi}|_{\xi=0} = 0 \quad (17)$$

The measurements are

$$y(t) = x(t,0) \qquad t = 1,2... \quad (18)$$

Letting $X(s,\xi)$ be the Laplace of $x(t,\xi)$ with respect to t for fixed ξ. Then (15) to (17) take the form

$$\begin{aligned} sX(s,\xi) &= \kappa X''(s,\xi) \\ X'(s,L_p) &= KU(s) \\ X'(s,0) &= 0 \end{aligned} \quad (19)$$

Prime and double prime here denote differentiation with respect to ξ, and $U(s)$ is the Laplace transform of $u(t)$. Solving (19) for fixed s gives

$$X(s,\xi) = A(s)e^{-\xi\sqrt{s/\kappa}} + B(s)e^{\xi\sqrt{s/\kappa}} \quad (20)$$

where the constants $A(s)$ and $B(s)$ are determined from the boundary values

$$X^{'}(s,0) = 0$$
$$X^{'}(s,L_p) = KU(s)$$

witch gives

$$A(s) = B(s) = \frac{KU(s)}{\sqrt{s/\kappa}(e^{L_p\sqrt{s/\kappa}}) - e^{-L_p\sqrt{s/\kappa}})} \quad (21)$$

Inserting this into (18) gives

$$Y(s) = X(s,0) = G_c(s)U(s) \quad (22)$$
$$G_c(s) = \frac{2KU(s)}{\sqrt{s/\kappa}(e^{L_p\sqrt{s/\kappa}} - e^{-L_p\sqrt{s/\kappa}})} \quad (23)$$

At this point, has been presented the two transfer functions that represent the dynamic response of the system. Eq. 14 shows the dynamic model of the thermoelectric system and Eq. 23 shows the heat transfer dynamic model by the plate.

In Eq. 14 the system has an infinite-order. For control purposes, a model reduction can be made. In this paper, the dynamic model of the thermoelectric cooler had been approximated by a first-order plus time-delay model (FOPTD) and the heat transfer by a transport delay.

4. EXPERIMENTS DESCRIPTION

4.1 Identification of FOPTD Model from a Step Input

An open-loop step response experiment is performed on the process and a FOPTD model $G(s) = \frac{K_p}{1+sT_p}e^{-s\tau_d}$ is estimated using the procedure presented in (Coelho and Barros [2003]).

4.2 Standard Relay Experiment - Gain Margin Estimate

A standard relay test presented in (Åström and Hägglund [1995]) is used to estimate the critical point and frequency. For most types of processes, a relay with amplitude d in an unit closed loop feedback leads to limit cycle operation, with oscillation conditions given by $G(j\omega_\pi) \cong m = -\frac{\pi a}{4d}$, where ω_π the critical frequency and a the process output amplitude.

It can be shown (Schei [1994]) that if this relay test is applied to a closed loop system, with transfer function $T(s)$, the limit cycle occurs at the closed loop critical frequency and the gain margin can be computed from the loop gain

$$L(j\omega_{gm}) = G(j\omega_{gm})C(j\omega_{gm}) \cong \frac{m}{1-m}. \quad (24)$$

4.3 Loop-Gain Relay Experiment - Phase Margin Estimate

A general relay procedure to estimate the frequency point for which a given transfer function has a desired gain is presented in (de Arruda and Barros [2003a]). The feedback structure applied for loop-gain experiment is presented in Fig.6. The conditions of the limit cycle operation are defined by the following proposition, with proof found in (de Arruda and Barros [2003a]):

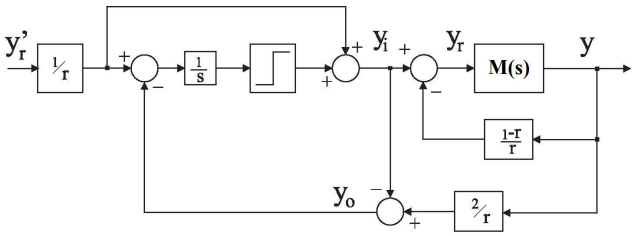

Fig. 6. Loop Gain Transfer Function Estimation.

Proposition 1. Consider a stable closed loop $M(s)$, with Loop-Gain $L(s)$, and a real positive number r so that the transfer function

$$F(s) = \frac{2}{r}\frac{M(s)}{M(s)\left(\frac{1-r}{r}\right)+1} - 1 \quad (25)$$

is also stable. Then if a limit cycle is present it oscillates at a frequency ω_o such that

$$|L(j\omega_o)| \approx r\,. \quad (26)$$

This procedure allows the estimation of the frequency at which the loop transfer function magnitude is close to r. Here $r = 1$ will be used, so that a limit cycle develops at the loop-gain crossover frequency. The phase margin can be estimated and used for stability evaluation and controller redesign.

4.4 Relay Based Gain and Phase Margins Redesign

The closed-loop performances are evaluated here on the phase and gain margins sense using the relay estimators previously described. This information is used to redesign the controllers as proposed in (de Arruda and Barros [2003b])

The problem is summarized as follows: given the closed loop system, how one can redesign the controller in such way that a new phase and gain margin specifications can be achieved. This problem is solved using a iterative approach applied to the following equations:

$$\angle G(j\omega_u)C(j\omega_u) = -\pi, \quad (27)$$
$$|G(j\omega_u)C(j\omega_u)| = \frac{1}{A_m}, \quad (28)$$
$$|G(j\omega_g)C(j\omega_g)| = 1 \quad (29)$$
$$\angle G(j\omega_g)C(j\omega_g) = -\pi + \phi_m. \quad (30)$$

where A_m is the desired gain margin and ϕ_m the desired phase margin. The iterative algorithm is used such that it only requires the knowledge of the frequencies ω_u and ω_g at each iteration. These frequencies are the solutions to Eqs. (27) and (29), and estimates are obtained using the relay experiments previously described. This algorithm uses the following lemmas to update the controller's parameters.

Controller Redesign for Gain Margin: The controller gain can be calculated for achieving the gain margin A_m using Eq. (28). That is, with the current gain margin,

GM^k, and the critical frequency, ω_u^k, one can compute the controller proportional gain, $\bar{K}_c^{k+1}$, from

$$\bar{K}_c^{k+1} = \frac{K_c^k GM^k}{A_m} \ . \tag{31}$$

Controller Redesign for Phase Margin: The controller gain can be calculated for achieving the phase margin ϕ_m using Eq. (30). This step is separated into two parts:

(1) Determine T_i^{k+1} such that Eq. (30) is satisfied, i.e.,

$$T_i^{k+1} = \frac{\tan\left[-\pi + \phi_m - PM^k + \tan^{-1}\left(\omega_g^k T_i^k\right)\right]}{\omega_g^k} \ . \tag{32}$$

The phase contribution from the PI controller ranges from $-90°$ to $0°$, and this information must be used in order to avoid invalid values of T_i^{k+1}. Since $\angle G\left(j\omega_g^k\right) + \angle C^{k+1/2}\left(j\omega_g^k\right) = -180° + \phi_m$, then the following condition must be satisfied in the above steps

$$-180° + \phi_m < \angle G\left(j\omega_g^k\right) < -90° + \phi_m \ , \tag{33}$$

If Eq. (33) is not satisfied, stop the iteration.

(2) Now, update the controller proportional gain K_c^{k+1} such that the loop gain at the frequency ω_g^k is equal to one,

$$K_c^{k+1} = \bar{K}_c^{k+1} \frac{\sqrt{\left(1/T_i^k\right)^2 + \omega_g^2}}{\sqrt{\left(1/T_i^{k+1}\right)^2 + \omega_g^2}} \ . \tag{34}$$

The controller at the end of the iteration is finally given by

$$C^{k+1} = K_c^{k+1}\left(\frac{s + 1/T_i^{k+1}}{s}\right) \ . \tag{35}$$

5. EXPERIMENTAL RESULTS

5.1 SISO - smaller time delay

The FOPTD model estimated from an open loop process step response experiment is

$$G(s) = \frac{1.145}{1 + 119.37s} e^{-18s} \tag{36}$$

There exists several design techniques based on a FOPTD model (Åström and Hägglund [1995]). Consider the Cohen-Coon (CC) method. In this technique the PI/PID controller is designed based on the parameters τ_d, T_p, K_p and $\Theta = \frac{\tau_d}{T_p}$ (see Table 1). A PI controller is designed.

$$C_{ccpi}(s) = 5.28(1 + \frac{1}{45.26s}).$$

Table 1. Cohen-Coon Method Parameters

Controller	K_c	T_i	T_d
PI	$\frac{1}{K_p}(0.083 + \frac{0.9}{\Theta})$	$\frac{3.3+0.31\Theta}{1+2.2\Theta}\tau_d$	-

The closed-loop step response is shown in Figure 7 The closed-loop performance is evaluated here on the phase (PM) and gain margins (GM) sense using the Standard

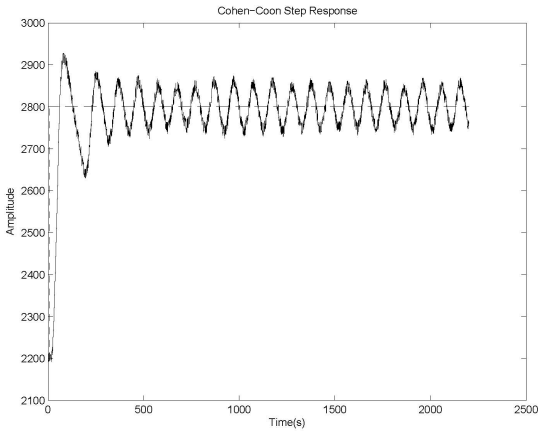

Fig. 7. Cohen-Coon Controller Closed Loop Step Response.

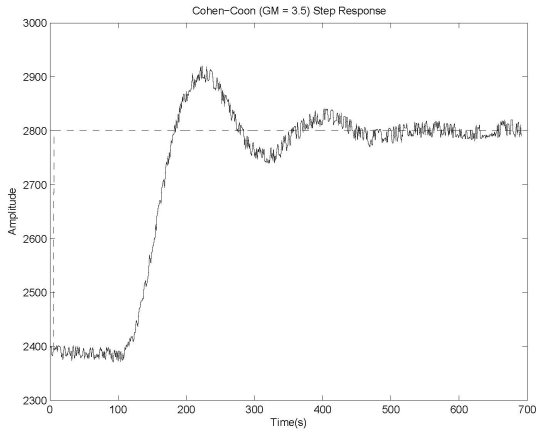

Fig. 8. Redesigned Cohen-Coon Controller Closed Loop Step Response GM = 3.5.

Relay and Loop Gain Experiments. The margins estimated for the closed-loop with CC PI controller are

$$GM = 1.051, and \quad PM = 79.97.$$

This information is used to redesign the controllers as proposed in (de Arruda and Barros [2003b]). The controller redesign for $GM = 3.5$ is

$$C_{ccRedesign}(s) = 1.48(1 + \frac{1}{41.307s}).$$

The step response for the new closed-loop is shown in Figure 8. As expected, the controller redesign in the direction of increasing the gain margin yields a more stable closed-loop.

5.2 SISO - larger time delay

An open loop process step response experiment is performed on the process and a FOPTD model is estimated using the same procedure.

$$K_p = 0.449, \quad T_p = 154.61s, and \quad \tau_d = 54s.$$

Using Ziegler-Nichols step response method the PI/PID controller is designed (see Table 2).

$$C_{znpi}(s) = 5.74(1 + \frac{1}{162s}).$$

Table 2. Ziegler-Nichols Method Parameters

Controller	K_c	T_i	T_d
PI	$\frac{0.9}{K_p\Theta}$	$3\tau_d$	-

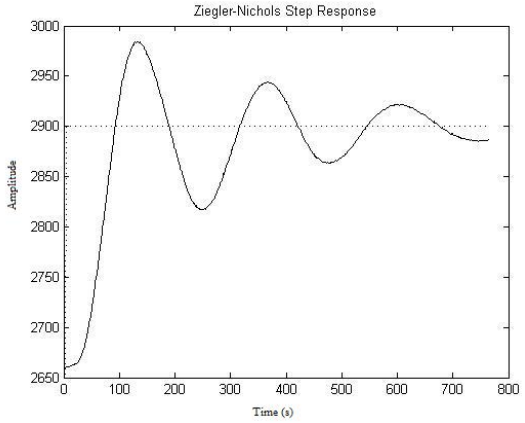

Fig. 9. Ziegler-Nichols Controller Closed Loop Step Response.

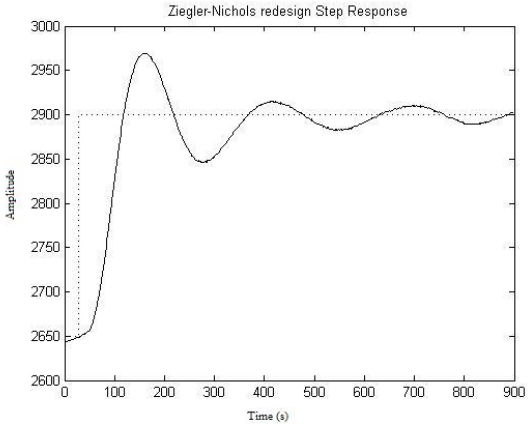

Fig. 10. Redesigned Ziegler-Nichols Controller Closed Loop Step Response GM = 3.5.

The step response for the closed loop with this controller is shown in Figure 9. The margins estimated for the closed-loop with CC PI controller are $GM = 1.66$ and $PM = 61.73$.

The controller redesign for $GM = 2.5$ and $PM = 70$ is $C_{znRedesign}(s) = 3.82(1 + \frac{1}{217s})$. The step response for the new closed-loop is shown in Figure 10.

5.3 TITO configuration

Step Tests sequentially applied to TITO process is performed (Figure 11) and a 2x2 FOPTD model is estimated using the same identification method presented in (Coelho and Barros [2003]) for SISO process.

$$\hat{G}(s) = \begin{bmatrix} \frac{1.186}{1+s99.36}e^{-12.58s} & \frac{0.83}{1+s166.76}e^{-29s} \\ \frac{0.66}{1+s124.76}e^{-48s} & \frac{2.36}{1+s109}e^{-5.86s} \end{bmatrix}$$

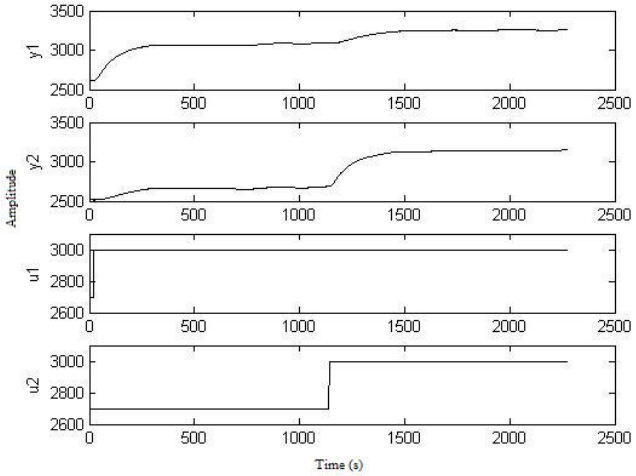

Fig. 11. Sequentially Step Test.

6. CONCLUSION

In control engineering courses, a laboratory experience that complements theoretical lecture material is essencial for students. In this way, a laboratory-scale temperature system and a set of experiments have been presented. The laboratory system is used in Control and Automation courses at DEE/UFCG.

REFERENCES

K. J. Åström and T. Hägglund. *PID Controllers: Theory, Design and Tuning*. Instrument Society of America, Research Triangle Park, North Carolina, 2nd edition, 1995.

F. S. Coelho and P. R. Barros. Continuous-time identification of first-order plus dead-time models from step response in closed loop. Rotterdam (The Netherlands), 2003. 13th IFAC Symposium on System Identification.

G. H. M. de Arruda and P. R. Barros. Relay-based closed loop transfer function frequency points estimation. *Automatica*, 39(2):309–315, 2003a.

G. H. M. de Arruda and P. R. Barros. Relay based gain and phase margins PI controller design. *IEEE Transctions on Inst. and Meas. Tech.*, 52(5):1548– 1553, 2003b.

H. J. Goldsmid. *Electronic Refrigeration*. Prentice-Hall, Inc, Englewood Cliffs (NJ), 1986.

B. J. Huang and C. L. Duang. System dynamic model and temperature control of a thermoelectric cooler. *International Journal of Refrigeration*, 23:197–207, 2000.

Kin ichi Uemura. Commercial peltier modules. In D. M. Rowe, editor, *CRC Handbook of Thermoelectrics*, pages 621–631. CRC Press, 1995.

L. Ljung. *System Identification - Theory for the User*. Prentice-Hall, Inc, Upper Saddle River (NJ), 1999.

S. B. Riffat and X. Ma. Thermoelectrics: a review of present and potential applications. *Applied Thermal Engineering*, 23:913–935, 2003.

T. S. Schei. Automatic tuning of PID controllers based on transfer function estimation. *Automatica*, 10:1983–1989, 1994.